

Characterization of the $\gamma\delta$ T-cell compartment during infancy reveals clear differences between the early neonatal period and 2 years of age

Marieke van der Heiden^{1,a}, Sophia Björkander^{1,a}, Khaleda Rahman Qazi¹, Julia Bittmann¹, Lena Hell¹, Maria C Jenmalm², Giovanna Marchini³, David Vermijlen⁴, Thomas Abrahamsson⁵, Caroline Nilsson^{6,7} & Eva Sverremark-Ekström¹

1 Department of Molecular Biosciences, The Wenner-Gren Institute, Stockholm University, Stockholm, Sweden

2 Department of Clinical and Experimental Medicine, Linköping University, Linköping, Sweden

3 Department of Women's and Children's Health, Karolinska Institutet, Stockholm, Sweden

4 Department of Pharmacotherapy and Pharmaceutics and Institute for Medical Immunology, Université Libre de Bruxelles, Bruxelles, Belgium

5 Department of Clinical and Experimental Medicine and Department of Paediatrics, Linköping University, Linköping, Sweden

6 Sachs' Children and Youth Hospital, Södersjukhuset, Stockholm, Sweden

7 Department of Clinical Science and Education, Södersjukhuset, Karolinska Institutet, Stockholm, Sweden

Keywords

childhood immunity, CMV, cord blood, neonatal immunity, prematurity, $\gamma\delta$ T cells

Correspondence

Eva Sverremark-Ekström, Department of Molecular Biosciences, The Wenner-Gren Institute, Stockholm University, Svante Arrheniusväg 20C, 106 91 Stockholm, Sweden.

E-mail: eva.sverremark@su.se

^aEqual Contributors.

Received 16 September 2019; Revised 31 October 2019; Accepted 1 November 2019

doi: 10.1111/imcb.12303

Immunology & Cell Biology 2020; **98**: 79–87

Abstract

$\gamma\delta$ T cells are unconventional T cells that function on the border of innate and adaptive immunity. They are suggested to play important roles in neonatal and infant immunity, although their phenotype and function are not fully characterized in early childhood. We aimed to investigate $\gamma\delta$ T cells in relation to age, prematurity and cytomegalovirus (CMV) infection. Therefore, we used flow cytometry to characterize the $\gamma\delta$ T-cell compartment in cord blood and peripheral blood cells from 14-day-, 2-year- and 5-year-old children, as well as in peripheral blood samples collected at several time points during the first months of life from extremely premature neonates. $\gamma\delta$ T cells were phenotypically similar at 2 and 5 years of age, whereas cord blood was divergent and showed close proximity to $\gamma\delta$ T cells from 14-day-old neonates. Interestingly, 2-year-old children and adults showed comparable $V\delta 2^+$ $\gamma\delta$ T-cell functionality toward both microbial and polyclonal stimulations. Importantly, extreme preterm birth compromised the frequencies of $V\delta 1^+$ cells and affected the functionality of $V\delta 2^+$ $\gamma\delta$ T cells shortly after birth. In addition, CMV infection was associated with terminal differentiation of the $V\delta 1^+$ compartment at 2 years of age. Our results show an adult-like functionality of the $\gamma\delta$ T-cell compartment already at 2 years of age. In addition, we demonstrate an altered $\gamma\delta$ T-cell phenotype early after birth in extremely premature neonates, something which could possibly contribute to the enhanced risk for infections in this vulnerable group of children.

INTRODUCTION

$\gamma\delta$ T cells are unconventional T cells, expressing the $\gamma\delta$ T-cell receptor (TCR).^{1,2} The activation of $\gamma\delta$ T cells is non-major-histocompatibility-complex restricted and these cells can also act as antigen presenting cells, suggesting that $\gamma\delta$ T cells act on the border of innate and adaptive immunity.^{3–6} $\gamma\delta$ T cells represent 0.5–10% of

the total circulating lymphocyte population in human adults.^{1,7,8} These $\gamma\delta$ T cells are suggested to play important roles in neonatal and infant immunity.^{1,7,9,10}

$\gamma\delta$ T cells can be further divided into several subsets, based on their γ - and δ - chain TCR usage. The most abundant subset in peripheral blood expresses the γ -chain variable region 9 ($V\gamma 9$) and δ -chain variable region 2 ($V\delta 2$). These $V\gamma 9^+V\delta 2^+$ cells are perceived to develop in

early life and to remain relatively stable until old age.^{9,11,12} This $\gamma\delta$ T-cell subset responds to phosphoantigens, such as (E)-4-hydroxy-3-methyl-but-2-enyl pyrophosphate (HMB-PP), derived from both gram-negative and gram-positive bacteria. Consequently, this subset is important in protection against bacterial infections.¹⁻³

Other $\gamma\delta$ T-cell subtypes, of which the majority is $V\delta 1^+$, are associated with mucosal immunity but can also be found in the periphery.^{2,3,13} Current knowledge suggests that $V\delta 1^+$ $\gamma\delta$ T cells develop toward the end of gestation and decrease in frequency toward adulthood.^{9,14} Besides absence of consensus on the activating ligands, cytomegalovirus (CMV) infection has shown to influence this subtype, both during adulthood and *in utero*.^{11,15-19} In addition, mucosal $V\delta 1^+$ $\gamma\delta$ T cells might play a role in regulating immunoglobulin E-mediated allergies, where they are believed to recognize allergens presented by $CD1^+$ dendritic cells.^{13,20}

Several reports describe $\gamma\delta$ T cells during gestation and adulthood, whereas these cells are not fully characterized during early childhood. However, a recent study analyzed the association between nongenetic factors and a broad range of immune dynamics in early childhood and found that CMV and prematurity were associated with an altered $\gamma\delta$ T-cell compartment during childhood.²¹ But how age and prematurity connect with the $\gamma\delta$ T-cell compartment during the first weeks and months of life, also considering differentiation and functionality, is not known. Therefore, we investigated the phenotype and function of the $V\delta 1^+$ and $V\delta 2^+$ $\gamma\delta$ T-cell subsets, using samples from cord blood (CB), and peripheral blood samples of 14-day-old neonates, 2- and 5-year-old children as well as from the first months of life from extremely preterm (PT) neonates.

The results show that CB $\gamma\delta$ T cells closely mimic the phenotype present during the first weeks of life and that there are clear effects of PT birth on the neonatal $\gamma\delta$ T-cell compartment. We further demonstrate that the $\gamma\delta$ T-cell compartment in 2-year-old children is both phenotypically and functionally mature and is clearly influenced by CMV serostatus. Together, our results enhance our understanding of $\gamma\delta$ T-cell immunity at young age and potentially of childhood immune protection.

RESULTS

Two-year-old children possess a mature $\gamma\delta$ T-cell compartment

The peripheral $\gamma\delta$ T-cell pool was investigated in cord blood mononuclear cells (CBMCs; called CB in figures) and peripheral blood mononuclear cells (PBMCs) derived from 2- and 5-year-old children. The frequencies of $\gamma\delta$ T cells (Figure 1a), $V\delta 1^+$ $\gamma\delta$ T cells (Figure 1b) and $V\delta 2^+$

$\gamma\delta$ T cells among $CD3^+$ cells (Figure 1c) were strikingly similar at 2 and 5 years of age, which was also reflected in an equal $V\delta 1^+$ over $V\delta 2^+$ ratio (Figure 1d). By contrast, besides the near absence of $V\delta 2^+$ $\gamma\delta$ T cells in CB (Figure 1c), CB possessed elevated frequencies of $V\delta 1^+ V\delta 2^-$ cells as compared with blood samples from both 2- and 5-year-old children (Figure 1e). Moreover, 2- and 5-year-old children showed similar frequencies of $V\gamma 9$ -expressing cells, both within the total $CD3^+$ compartment and among the $V\delta 1^+$ and $V\delta 2^+$ $\gamma\delta$ T-cell subsets, which clearly deviated in CB (Figure 1f-h).

The 2- and 5-year-old children possessed a significantly lower frequency of cells expressing the differentiation markers CD27 and CD28 in both the $V\delta 1^+$ (Figure 2a-c) and $V\delta 2^+$ (Figure 2d-f) compartments as compared with CB, indicating a clear differentiation of these cells already at 2 years of age. To verify whether this differentiation of the $V\delta 2^+$ subset was associated with the acquisition of a functional response, we verified the interferon γ (IFN γ) production after stimulation with either a microbial (HMB-PP) or a polyclonal (CD3:CD28 beads) activator. The $V\delta 2^+$ subset at 2 years of age showed an equal frequency of IFN γ^+ cells as adult $V\delta 2^+$ cells upon both types of stimulations (Figure 2g, h).

The $\gamma\delta$ T-cell population is functionally compromised during the early neonatal period

Based on the notable differences in $\gamma\delta$ T-cell subsets between CBMCs and PBMCs from 2-year-old children, we extended our analysis with PBMCs from 14-day-old neonates. The principal component analysis (Figure 3a) revealed that the $\gamma\delta$ T-cell compartment in 14-day-old neonates (blue) was closely related to that of CB (red). The $\gamma\delta$ T cells from 14-day-old neonates and 2-year-old children (yellow) were clearly separated, which was mostly based on higher frequencies of $V\delta 2^+$ $\gamma\delta$ T cells in the 2-year-old children. Importantly, although stimulation with HMB-PP enhanced the percentage of IFN $\gamma^+ V\delta 2^+$ cells in the 14-day-old neonates, the response was significantly lower than that at 2 years of age (Figure 3b). Interestingly, TCR-mediated stimulation with CD3:CD28 beads induced a robust IFN γ response in the $V\delta 2^+$ $\gamma\delta$ T cells from 14-day-old neonates, a response that was statistically higher than that from the 2-year-old children (Figure 3c).

$\gamma\delta$ T cells are significantly affected by prematurity

We next investigated the effect of prematurity on the $\gamma\delta$ T-cell composition and functionality shortly after birth. CBMCs and PBMCs (collected 14 days, 28 days and at a timepoint corresponding to postmenstrual week 36) from

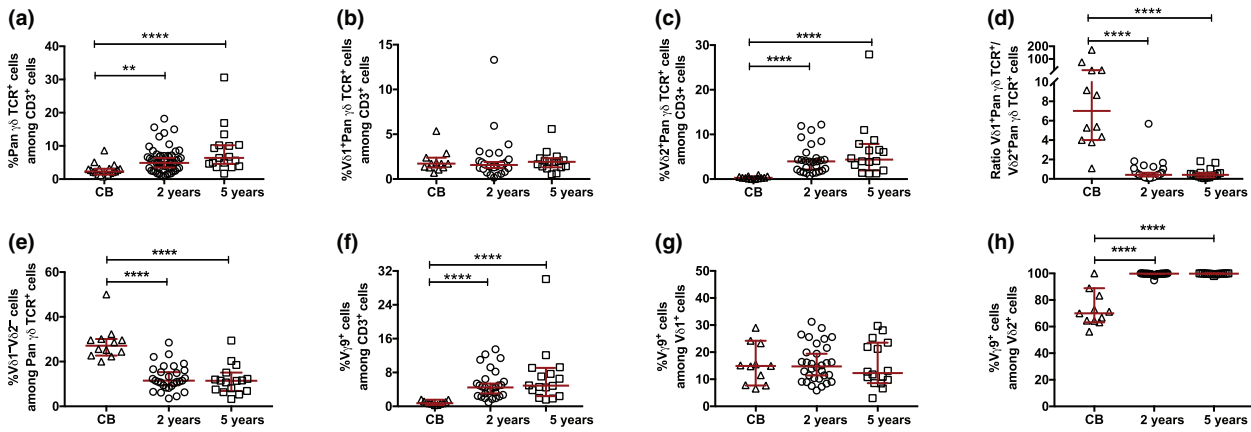


Figure 1. The frequency of $\gamma\delta$ T-cell subsets in cord blood (CB) mononuclear cells (CBMCs) and peripheral blood mononuclear cells (PBMCs) from 2- and 5-year-old children. (a) The frequencies of Pan $\gamma\delta$ TCR $^+$ cells among CD3 $^+$ cells in CBMCs (CB; $n = 19$) and PBMCs from 2-year-old ($n = 52$) and 5-year-old ($n = 16$) children. The frequencies of (b) V δ 1 $^+$ Pan $\gamma\delta$ TCR $^+$ cells among CD3 $^+$ cells, (c) V δ 2 $^+$ Pan $\gamma\delta$ TCR $^+$ cells among CD3 $^+$ cells, (d) the V δ 1 $^+$ Pan $\gamma\delta$ TCR $^+$ /V δ 2 $^+$ Pan $\gamma\delta$ TCR $^+$ cell ratio, (e) V δ 1 $^-$ V δ 2 $^-$ cells among Pan $\gamma\delta$ TCR $^+$ cells, (f) V γ 9 $^+$ cells among CD3 $^+$ cells, (g) V γ 9 $^+$ cells among V δ 1 $^+$ cells and (h) V γ 9 $^+$ cells among V δ 2 $^+$ cells in CB ($n = 12$) and in PBMCs from 2- ($n = 28$) and 5- ($n = 16$) year-old children. TCR, T-cell receptor. ** $P < 0.01$, **** $P < 0.0001$. Data are combined from a minimum of 20 independent experiments.

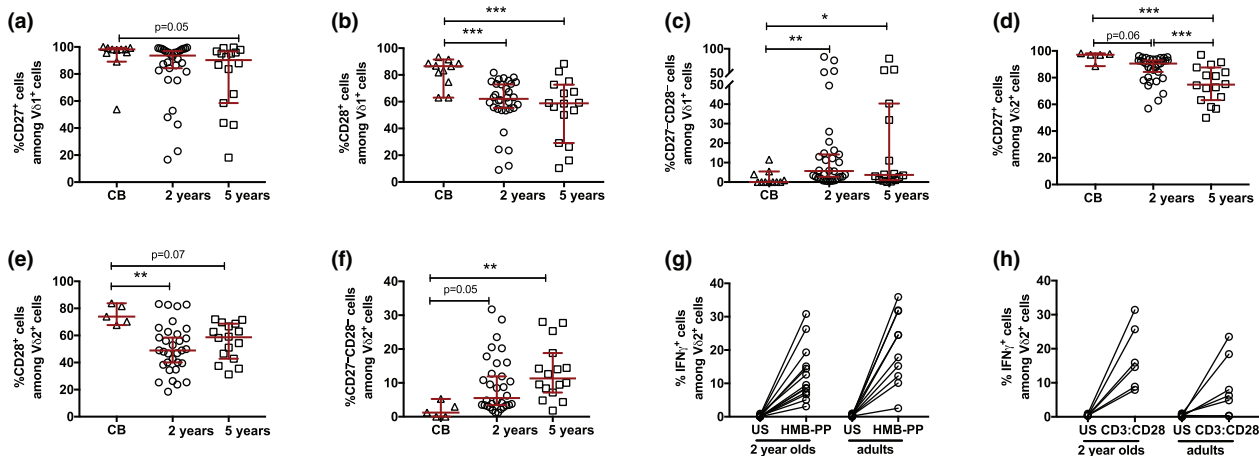


Figure 2. The differentiation and functionality of $\gamma\delta$ T cells in cord blood (CB) and peripheral blood mononuclear cells (PBMCs) from 2- and 5-year-old children. The frequencies of (a) CD27 $^+$ cells among V δ 1 $^+$ cells, (b) CD28 $^+$ cells among V δ 1 $^+$ cells and (c) CD27 $^-$ CD28 $^-$ cells among V δ 1 $^+$ cells. The frequencies of (d) CD27 $^+$ cells among V δ 2 $^+$ cells, (e) CD28 $^+$ cells among V δ 2 $^+$ cells and (f) CD27 $^-$ CD28 $^-$ cells among V δ 2 $^+$ cells in CB ($n = 12$) and in PBMCs from 2- ($n = 28$) and 5- ($n = 16$) year-old children. The frequency of IFN γ $^+$ cells among V δ 2 $^+$ cells after 24-h stimulation with (g) (E)-4-hydroxy-3-methyl-but-2-enyl pyrophosphate (HMB-PP) or (h) CD3:CD28 beads in PBMCs from 2-year-old children ($n = 13$ and $n = 6$, respectively) and adults ($n = 10$ and $n = 7$, respectively). * $P < 0.05$, ** $P < 0.01$, *** $P < 0.001$. Data are combined from a minimum of 10 independent experiments. IFN, interferon; US, unstimulated.

premature extremely low gestational age neonates (ELGAN) with extremely low birthweight (ELBW) are referred to as PT. Premature birth significantly affected the frequencies of V δ 1 $^+$ $\gamma\delta$ T cells (Figure 4a), whereas the frequencies of V δ 2 $^+$ $\gamma\delta$ T cells (Figure 4b) and V δ 1 $^-$ V δ 2 $^-$ $\gamma\delta$ T cells (Figure 4c) were similar to the full-term 14-day-old neonates. Furthermore, the frequency of V δ 1 $^+$ $\gamma\delta$ T cells was significantly lower in the PT CB samples

(Figure 4d), whereas a trend to a higher frequency of V δ 2 $^+$ $\gamma\delta$ T cells was observed (Figure 4e). The V δ 1 $^+$ $\gamma\delta$ T-cell phenotype clearly differed between the ELGAN/ELBW neonates at postmenstrual week 36 as compared with the 14-day-old neonates, which was mainly related to a higher expression of CD27 and CD28 (Figure 4g).

Despite similar frequencies of the V δ 2 $^+$ cells in ELGAN/ELBW and 14-day-old neonates, phenotypical differences in

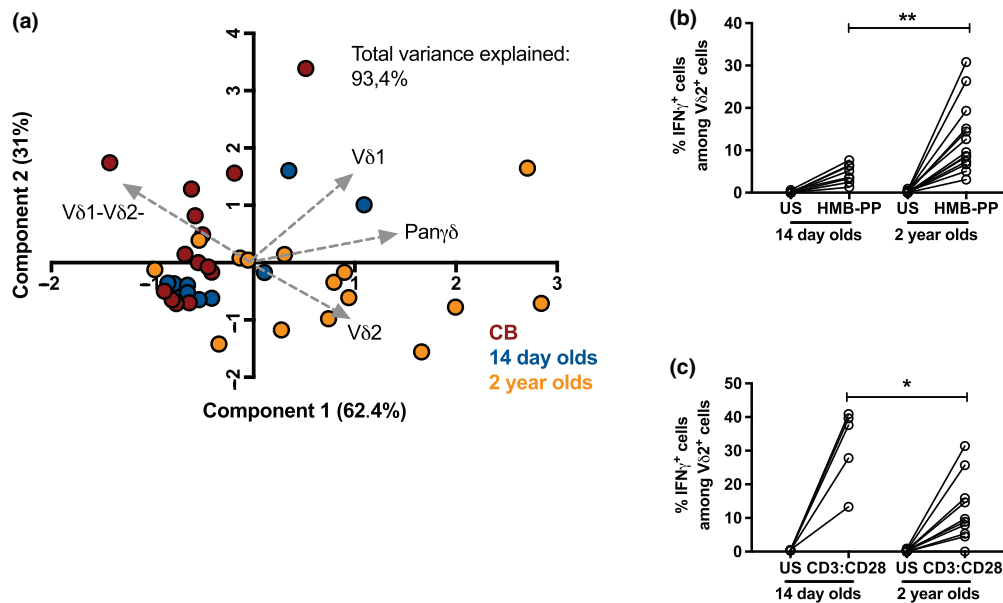


Figure 3. The $\gamma\delta$ T-cell compartment in peripheral blood mononuclear cells (PBMCs) from 14-day-old neonates. **(a)** Principal component analysis (PCA) comparing the $\gamma\delta$ T-cell phenotype of cord blood (CB; red; $n = 12$), 14-day-old neonates (blue; $n = 10$) and 2-year-old children (yellow; $n = 17$). The total frequencies of P α $\gamma\delta$ TCR⁺ cells among CD3⁺ cells as well as the frequencies of V δ 2⁺P α $\gamma\delta$ TCR⁺ cells among CD3⁺ cells, V δ 1⁺P α $\gamma\delta$ TCR⁺ cells among CD3⁺ cells and V δ 1⁻ V δ 2⁻ cells among P α $\gamma\delta$ TCR⁺ cells were included in the PCA. The frequency of IFN γ ⁺ cells among V δ 2⁺ cells after 24-h stimulation with **(b)** (E)-4-hydroxy-3-methyl-but-2-enyl pyrophosphate (HMB-PP) or **(c)** CD3:CD28 beads between the 14-day-old neonates ($n = 8$ and $n = 5$, respectively) and 2-year-old children ($n = 13$ and $n = 10$, respectively). **P* < 0.05, ***P* < 0.01. Data are combined from a minimum of 10 independent experiments. IFN, interferon; TCR, T-cell receptor; US, unstimulated.

the V δ 2 compartment at 14 days after birth were observed (Figure 4h). This difference was mostly explained by lower frequencies of V δ 2⁺ cells that express V γ 9 (Figure 4i) and granzyme B (Figure 4j) in the ELGAN/ELBW PT neonates, which converged to the pattern found in the 14-day-old neonates at the later timepoints. Interestingly, HMB-PP and CD3:CD28 bead stimulation induced a comparable frequency of IFN γ ⁺V δ 2⁺ cells in the ELGAN/ELBW PT neonates at postmenstrual week 36 as compared with the 14-day-old neonates (Figure 4k, l).

CMV infection is associated with a terminal differentiation of the V δ 1⁺ $\gamma\delta$ T-cell compartment already at 2 years of age

High variation was observed in the $\gamma\delta$ T-cell compartment at 2 years of age, which was possibly related to the genetic background and/or microbial exposure. We investigated whether infection with CMV, known to influence V δ 1⁺ $\gamma\delta$ T cells in adults and fetuses, is associated with the $\gamma\delta$ T-cell phenotype also at 2 years of age. The children were serotyped and divided as being either CMV⁻ and CMV⁺, based on the presence of CMV-specific antibodies. The V δ 1 compartment at 2 years of age was increased in frequency (Figure 5a) and showed a different phenotype

(Figure 5b) in CMV-infected infants. Specifically, the frequencies of V δ 1 cells with a terminally differentiated phenotype, CD27⁻CD28⁻ (Figure 5c), CD27⁻CD45RA⁺ (Figure 5d), CD57⁺ (Figure 5e), granzyme B⁺ (Figure 5f) and CD16⁺ (Figure 5g), were significantly enhanced in CMV-infected children. By contrast, the overall V δ 2 compartment did not diverge between CMV⁻ and CMV⁺ children (Supplementary figure 3).

DISCUSSION

Within this study, we demonstrate that 2- and 5-year-old children possess a mature $\gamma\delta$ T-cell phenotype, whereas the $\gamma\delta$ T-cell compartment in early postneonatal life (14 days after birth) is similar to CB. This maturity at 2 years of age is supported by comparable functional responses of the V δ 2⁺ compartment as in adults toward both a polyclonal (CD3:CD28 beads) and bacterial (HMB-PP) stimulation, while at 14 days after birth this functional response appears to be more restricted. Importantly, we show that extreme PT birth clearly affects the $\gamma\delta$ T-cell phenotype directly after birth, as $\gamma\delta$ T cells collected 14 days after birth from preterm neonates and full-term neonates display clear phenotypical differences. Finally, we show that early life

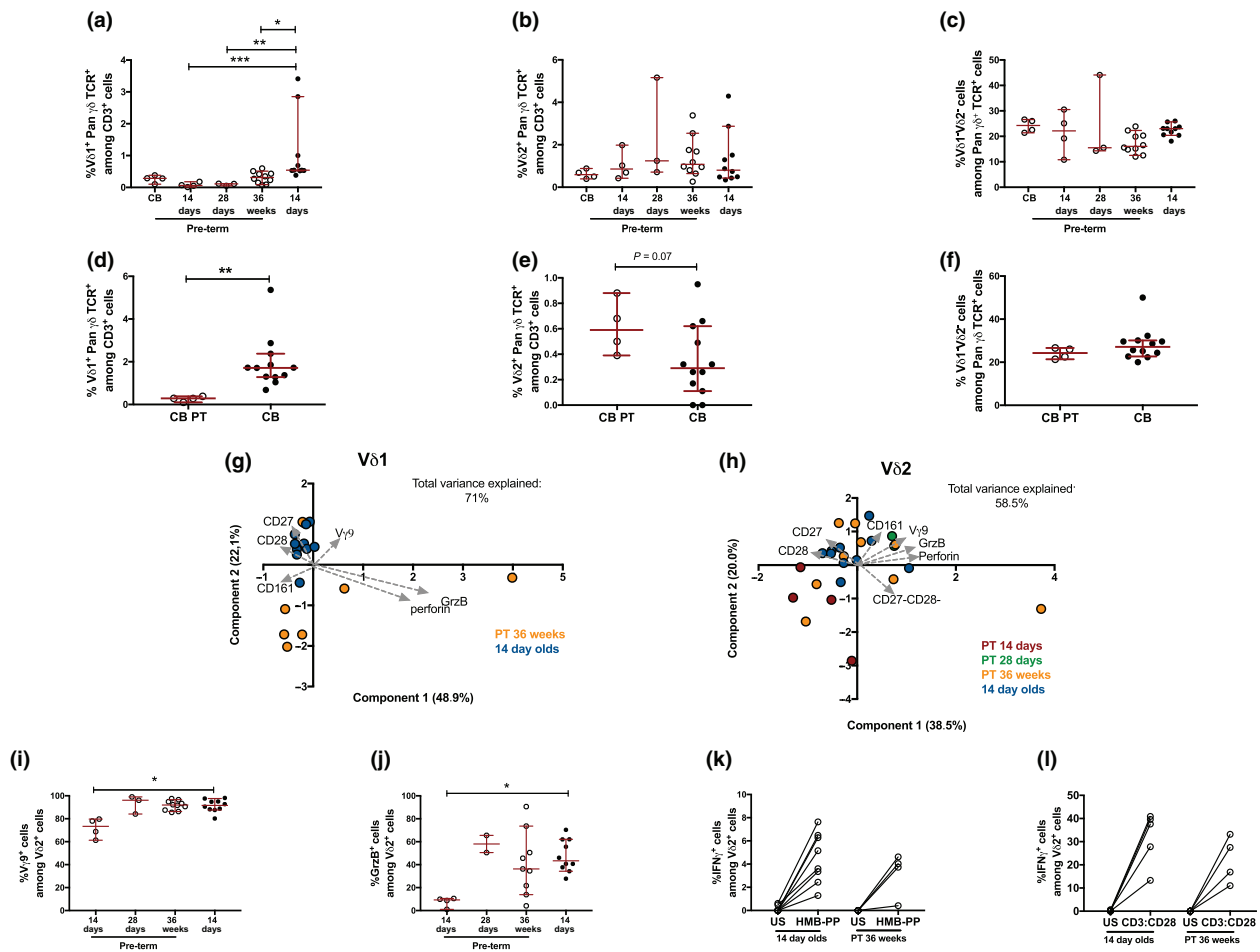


Figure 4. The $\gamma\delta$ T-cell phenotype and function in preterm neonates. The frequencies of (a) V δ 1⁺Pan $\gamma\delta$ TCR⁺ cells among CD3⁺ cells, (b) V δ 2⁺Pan $\gamma\delta$ TCR⁺ cells among CD3⁺ cells and (c) V δ 1⁻V δ 2⁻ cells among Pan $\gamma\delta$ TCR⁺ cells in 14-day-old full-term (FT) neonates ($n = 10$) and preterm (PT) neonates at different timepoints after birth [cord blood (CB; $n = 4$), 14 days ($n = 4$), 28 days ($n = 3$) and at postmenstrual age week 36 ($n = 10$)]. The frequencies of (d) V δ 1⁺Pan $\gamma\delta$ TCR⁺ cells among CD3⁺ cells, (e) V δ 2⁺Pan $\gamma\delta$ TCR⁺ cells among CD3⁺ cells and (f) V δ 1⁻V δ 2⁻ cells among Pan $\gamma\delta$ TCR⁺ cells in CB samples from preterm (CB PT, $n = 4$) and full-term CB samples (CB, $n = 12$). (g) Principal component analysis (PCA) comparing the V δ 1 phenotype between the full-term 14-day-old neonates (14-day-old, blue) and preterm neonates at postmenstrual week 36 (PT 36 weeks, yellow). The analysis includes the frequencies of CD27⁺, CD28⁺, CD161⁺, GrzB⁺, perforin⁺ and V γ 9⁺ cells among V δ 1⁺ cells. (h) PCA comparing the V δ 2 phenotype between the 14-day-old neonates (blue) and preterm (PT) newborns at 14 days (red), 28 days (green) and postmenstrual week 36 (yellow). The analysis includes the frequencies of CD28⁺, CD27⁺, CD27⁻CD28⁻, CD161⁺, GrzB⁺ and V γ 9⁺ cells among V δ 2⁺ cells. The frequencies of (i) V γ 9⁺ cells among V δ 2⁺ cells and (j) granzyme B (GrzB⁺) among V δ 2⁺ cells between 14-day-old neonates ($n = 10$) and PT neonates at different timepoints after birth [14 days ($n = 4$), 28 days ($n = 3$) and at postmenstrual age week 36 ($n = 10$)]. The frequency of IFN γ ⁺ cells among V δ 2⁺ cells after 24-h stimulation with (k) (E)-4-hydroxy-3-methyl-but-2-enyl pyrophosphate (HMB-PP) or (l) CD3:CD28 beads in the 14-day-old neonates ($n = 8$ and $n = 5$, respectively) and the preterm neonates at postmenstrual week 36 (PT 36 weeks; $n = 4$ and $n = 4$, respectively). * $P < 0.05$, ** $P < 0.01$, *** $P < 0.001$. Data are combined from a minimum of 5 independent experiments. TCR, T-cell receptor; US, unstimulated.

CMV infection associates with a distinct V δ 1⁺ $\gamma\delta$ T-cell phenotype at 2 years of age.

Although numerous studies investigate $\gamma\delta$ T cells during adulthood as well as during gestation, little is known about $\gamma\delta$ T cells in early childhood. We show that V δ 2⁺ $\gamma\delta$ T cells from 2-year-old children and adults are functionally comparable, suggesting mature responses of

the V δ 2⁺ compartment toward bacterial infections at 2 years of age,¹⁻³ which is in agreement with others.¹⁴ Interestingly, V δ 2⁺ cells were recently found to be resistant toward senescence at old age, suggesting a stable phenotype of these cells once the mature state is reached.¹¹ On the contrary, V δ 2⁺ cells are present at very low numbers at birth, a finding that is supported by

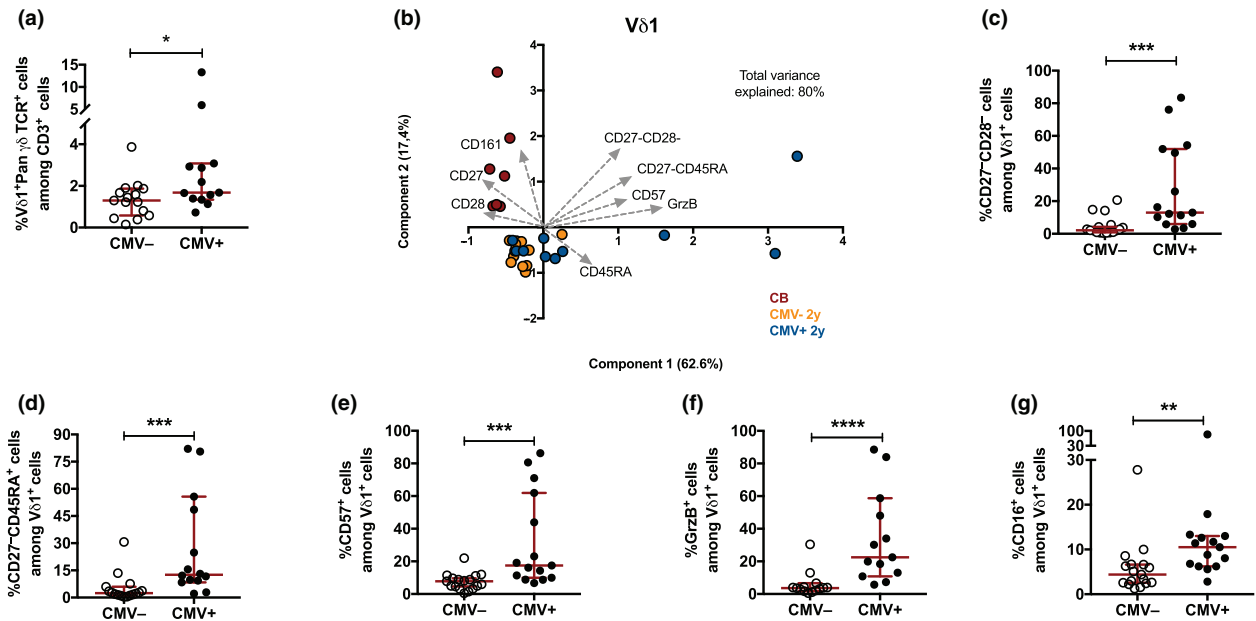


Figure 5. The $V\delta 1$ phenotype in cytomegalovirus (CMV) infected and noninfected 2-year-old children. **(a)** The frequency of $V\delta 1^+$ cells among $CD3^+$ cells in CMV- ($n = 17$) and CMV+ ($n = 15$) 2-year-old children. **(b)** Principal component analysis of the $V\delta 1$ phenotype comparing cord blood (red; $n = 7$), CMV negative (CMV-, yellow; $n = 12$) and CMV-infected (CMV+, blue; $n = 10$) 2-year-old children. The frequencies of $CD28^+$, $CD27^+$, $CD161^+$, $CD27^-CD28^-$, $CD27^-CD45RA^+$, $CD57^+$, $GrzB^+$, $CD16^+$, perforin $^+$, $CD158b^+$ and $CD45RA^+$ cells among the $V\delta 1^+$ cells are included in the analysis. The frequency of **(c)** $CD27^-CD28^-$, **(d)** $CD27^-CD45RA^+$, **(e)** $CD57^+$, **(f)** $GrzB^+$ and **(g)** $CD16^+$ cells among $V\delta 1^+$ cells in CMV- ($n = 17$) and CMV+ ($n = 15$) 2-year-old children. * $P < 0.05$, ** $P < 0.01$, *** $P < 0.001$; **** $P < 0.0001$. Data are combined from a minimum of 10 independent experiments.

others.^{1,14,22,23} We were able to show that CB samples do closely relate to peripheral samples derived 14 days after birth, indicating that CB is a representative sample when studying early life $\gamma\delta$ T cells. This finding could be $\gamma\delta$ T-cell specific, based on the recent report on CB not mirroring neonatal immunity for other immune cells.²⁴ Nevertheless, a small enhancement of the $V\delta 2^+$ $\gamma\delta$ T-cell frequency as well as an increased frequency of these cells expressing the $V\gamma 9$ chain is observed already 14 days after birth, suggesting a quick start of maturation as a result of microbial exposure.^{9,12,14} These $V\delta 2^+$ $\gamma\delta$ T cells at 14 days after birth show a developed capacity to produce $IFN\gamma$ after a TCR-mediated stimulation, while the response toward HMB-PP is more restricted, possibly indicating an immature response toward bacteria at this age.

Preterm birth clearly affects the $\gamma\delta$ T-cell phenotype 14 days after birth and possibly suggests that these cells mature toward the end of full-term gestation. This immature $V\delta 2^+$ phenotype in ELGAN/ELBW neonates might contribute to the higher bacterial infection burden in these vulnerable neonates²⁵ and align with earlier findings that immune cell immaturity is linked to prematurity.^{26,27} Subsequently, it is of interest to investigate these $V\delta 2^+$ $\gamma\delta$ T cells in a longitudinal

manner in a larger cohort of PT neonates. We demonstrate reduced frequencies of $V\delta 1^+$ $\gamma\delta$ T cells after extreme preterm birth, both shortly (14 days) after birth and at the timepoint equal to postmenstrual week 36. Notwithstanding, the $V\delta 1^+$ frequency tend to increase over time in the preterm neonates, indicating postgestational maturation of this compartment. These results are in agreement with findings of Vermijlen *et al.*⁹ showing sharp increases of $V\delta 1^+$ cells toward the end of full-term gestation, whereas their frequencies were low in gestational weeks 20–30, the gestational age window of our extreme preterm neonates.

Interestingly, CB samples and samples from 14-day-old neonates possess relatively high frequencies of $V\delta 1^-V\delta 2^-$ $\gamma\delta$ T cells than all other age groups. These cells might be classified as $V\delta 3^+$ or $V\delta 5^+$ and frequencies of these cells are known to decline with increasing age, which might be a result of homing to mucosal sites.^{9,23}

Finally, our results indicate that skewing of a large part of the $V\delta 1^+$ compartment toward a terminally differentiated, including high cytotoxic potential, phenotype is associated with CMV infection already at 2 years of age, which is similar to what has been reported for $\gamma\delta$ T cells in adults^{11,17,28} and older children.²⁹ Our results indicate that CMV infection in children affects the $\gamma\delta$ T cells in a similar

manner as to what is known about $\alpha\beta$ T cells^{30,31} and indicate strong antiviral activity of $\gamma\delta$ T cells already at the age of 2 years. Unfortunately, we are not able to determine functional CMV-specific responses, because the ligands of CMV-responsive $V\delta 1^+$ cells are unknown stress factors secreted by CMV-infected cells and consequently hard to mimic *in vitro*.^{15,18,28} In addition, our study is not powered to determine effects of CMV infection in the PT neonates, which would be of interest regarding results of Vermijlen *et al.*, showing clear effects of *in utero* CMV infection on the fetal $V\delta 1^+$ $\gamma\delta$ T-cell composition.³² Moreover, it would be valuable to determine the associations of Epstein-Barr virus, another potent herpesvirus, with the $V\delta 1^+$ $\gamma\delta$ T-cell phenotype.^{33,34} Future work could study CMV-mediated effects on $V\delta 1^+$ $\gamma\delta$ T cells in relation to clinical outcomes, such as infection burden and allergy development during early childhood.^{13,20}

In conclusion, we provide unique insights into the $\gamma\delta$ T-cell phenotype and function at several timepoints during early childhood. The $\gamma\delta$ T-cell compartment of PT infants is clearly affected 14 days after birth but becomes rapidly functional within a few months. Moreover, the $\gamma\delta$ T-cell compartment shows maturity at 2 years of age, including comparable functionality to the $V\delta 2^+$ $\gamma\delta$ T cells as in adults, both in functional responses of the $V\delta 2^+$ subtype and in the effects of CMV infection on the $V\delta 1^+$ subtype. These results contribute to a better understanding of $\gamma\delta$ T-cell immunity in early life, which is important for our knowledge on immune function and protection against infections at young age.

METHODS

Cohort material

CBMCs and PBMCs from different cohorts were combined in this study. CBMCs ($n = 19$; called CB in figures) and PBMCs from 2-year-old ($n = 52$) and 5-year-old ($n = 16$) children were randomly chosen from a prospective birth cohort, as described elsewhere.³⁵ All children were born at term between 1997 and 2000 in the Stockholm area and had birth weights within the normal range. This cohort was recruited at the Sachs' Children's Hospital and the study was approved by the Human Ethics Committee at Huddinge University Hospital, Stockholm (Dnr. 75/97, 33/02). All parents provided informed consent.

Moreover, CBMCs and PBMCs were used from a prospective, randomized-controlled, multicenter trial: PROPEL (*Prophylactic Probiotics to Extremely Low Birth Weight Premature Infants*). The study was executed in 10 neonatal units between 2012 and 2015 in the region of Stockholm and Linköping and is described in detail elsewhere.³⁶ The study was approved by the Ethics Committee for Human Research in Linköping (Dnr 2012/28-31, Dnr 2012/433-32). In short,

infants were eligible for participation between gestational week 23⁺⁰ and 27⁺⁶ and with a birthweight less than 1000 g. CBMCs ($n = 4$) and PBMCs from several timepoints after birth were used: 14 days ($n = 4$), 28 days ($n = 3$) and at postmenstrual week 36 ($n = 10$; all referred to as PT). In addition, PBMCs from full-term born children were collected 14 days after birth ($n = 10$; referred to as 14-day-old neonates).

Adult PBMCs ($n = 10$) were collected from healthy volunteers, which was approved by the Regional Ethics Committee at Karolinska Institute, Stockholm, Sweden (Dnr. 04-106/1 2014/2052-32). For all human material, the use of the samples was performed in accordance with General Data Protection Regulation and the correct explicit authorizations were obtained.

Cord and peripheral blood mononuclear cell isolation

Cord and peripheral blood was collected in collection tubes containing heparin (BD Biosciences Pharmingen, San Jose, CA, USA). CBMCs and PBMCs were isolated with gradient separation using Ficoll-Hypaque (GE Healthcare Bio-sciences AB, Uppsala, Sweden). The cells were washed using RPMI-1640 medium (GE Healthcare – HyClone Laboratories Inc., Logan, UT, USA) and thereafter frozen in freezing media containing 40% RPMI-1640, 50% fetal calf serum and 10% dimethyl sulfoxide (all from Sigma Aldrich, St Louis, MO, USA) and stored in liquid nitrogen until further use.

Processing and *in vitro* stimulation of PBMCs

Frozen CBMCs and PBMCs were thawed and washed with RPMI-1640 supplemented with 20 mM HEPES (GE Healthcare – HyClone Laboratories). The cells were counted and viability was assessed with Trypan Blue staining; only cells with sufficient viability were used for the functional assays. Subsequently, the cells were resuspended in a concentration of 10^6 cells mL^{-1} in cell culture medium, consisting of RPMI-1640 supplemented with 20 mM HEPES, 100 U mL^{-1} penicillin, 100 $\mu\text{g mL}^{-1}$ streptomycin, 2 mM L-glutamate (2 mM) (all GE Healthcare – HyClone Laboratories) and 10% heat-inactivated fetal calf serum (Sigma Aldrich). The cells were either rested for a minimum of 1 h before basal phenotypic staining or stimulated for 24 h with 40 ng mL^{-1} HMB-PP (Sigma Aldrich) or Dynabeads Human T-activator CD3:CD28 (Thermo Fisher Scientific, Waltham, MA, USA) at a 2:1 cell-to-bead ratio at 37°C and 5% CO₂ in a flat-bottomed 48-well plate (Costar, Cambridge, UK). Brefeldin A (BD Biosciences) was added during the last 4 h of incubation.

Flow cytometric analysis

The cells were washed with phosphate-buffered saline and stained with live/dead FVS780 (BD Biosciences) in phosphate-buffered saline, followed by a blocking step with 10% human serum in fluorescence-activated cell sorting wash buffer containing phosphate-buffered saline, 0.1% bovine serum albumin (Roche Diagnostics GmbH, Mannheim, Germany)

and EDTA (Invitrogen, Grand Island, NY, USA). Subsequently, the cells were surface stained with the following antibodies in fluorescence-activated cell sorting wash buffer: CD3-BV510 (Clone: UCHT-1), V δ 2-APC (Clone: B6) (both BioLegend, San Diego, CA, USA) and V δ 1-PE-Cy7 (Beckman Coulter, Brea, CA, USA) together with several combinations of the following antibodies: Pan $\gamma\delta$ TCR-FITC (Clone: Immu510), V γ 9-FITC (both Beckman Coulter), CD27-PE (Clone: M-T271), CD45RA-FITC (Clone: H1100), CD158b/j-PE (Clone: DX27) (all BioLegend), CD28-BV421 (Clone: CD28.2), CD57-FITC (Clone: NK-1) or CD16-BV421 (Clone: 3G8) (BD Biosciences). After surface staining, cells were either washed and fixed with 4% paraformaldehyde before analysis or treated with the intracellular staining fixation kit (BioLegend) according to the manufacturers' instructions. The cells were intracellularly blocked with 10% human serum and stained with Perforin-FITC (Clone: B-D48; BioLegend) and Granzyme B-V450 (Clone: GB-11; BD Biosciences) in intracellular staining perm/wash buffer (BioLegend). HMB-PP and CD3:CD28 beads-stimulated cells were intracellularly stained with IFN γ -PerCP Cy5.5 (Clone: B27; BD Biosciences). The data were acquired with a FACSVerser in combination with the FACSsuite software (BD Biosciences). Fluorescence-minus-one and isotype controls were used for gating. Example gating strategies are provided in Supplementary figures 1 and 2.

Detection of CMV infection status

CMV infection status was based on the presence of CMV immunoglobulin G antibodies in plasma samples. These immunoglobulin G antibodies were determined with an in-house CMV-immunoglobulin G ELISA described elsewhere.³⁷

Statistical analysis

All data were checked for normality distribution before statistical analysis. In all graphs, the median with 95% confidence interval is displayed. Three or more different age groups were compared with the Kruskal–Wallis test followed by Dunn's multiple comparisons test. The unstimulated and HMB-PP or CD3:CD28 beads-stimulated samples were compared with the Wilcoxon matched-pairs signed-rank test. Two different age groups or the CMV– and CMV+ groups were compared with the Mann–Whitney *U*-test. A *P*-value <0.05 was considered significant. Significances are indicated with **P* < 0.05, ***P* < 0.01, ****P* < 0.001, *****P* < 0.0001. For these analysis, GraphPad Prism V7 was used.

The principal components analyses were performed using SPSS version 25 and GraphPad Prism version 7. Different combinations of cell subset frequencies were used in this analysis, as mentioned in the figure legends. Data were reduced into two principal components, of which the amount of variance in the data that is explained by the component is mentioned as a percentage on the axes. In addition, the total variance in the data that is explained by the two principal components combined is indicated in the graphs. The validity of the principal components analyses was checked with the Kaiser–Meyer–Olkin measure of sampling adequacy and the

Bartlett test of sphericity. Subset frequencies that explained most variation, including the direction of the relation, were indicated with arrows in the plots. Different age groups are indicated with different colors, as explained in the figure legends.

ACKNOWLEDGMENTS

We thank all the participants and their parents for their cooperation and the nurses involved in blood drawings. This work was supported by The Swedish Research Council (2016-01715_3), the Torsten Söderberg Foundation, the Cancer and Allergy Foundation, the Swedish Asthma and Allergy Association's Research Foundation, the Hesselman Foundation, the Golden Jubilee Memorial Foundation, the Crownprincess Lovisa/Axel Tielman Foundations, the Engkvist Foundations, the Swedish Heart-Lung Foundation and the Hedlund Foundation.

CONFLICT OF INTEREST

All authors declare no conflict of interest.

REFERENCES

1. Vermijlen D, Prinz I. Ontogeny of innate T lymphocytes - some innate lymphocytes are more innate than others. *Front Immunol* 2014; **5**: 1–12.
2. Gao Y, Williams AP. Role of innate T cells in anti-bacterial immunity. *Front Immunol* 2015; **6**: 1–8.
3. Tyler CJ, Doherty DG, Moser B, et al. Human V γ 9/V δ 2 T cells: innate adaptors of the immune system. *Cell Immunol* 2015; **1**: 10–21.
4. Bonneville M, O'Brien RL, Born WK. $\gamma\delta$ T cell effector functions: a blend of innate programming and acquired plasticity. *Nat Rev Immunol* 2010; **10**: 467–478.
5. Lawand M, Déchanet-Merville J, Dieu-Nosjean MC. Key features of gamma-delta T-cell subsets in human diseases and their immunotherapeutic implications. *Front Immunol* 2017; **8**: 1–9.
6. Parker CM, Groh V, Band H, et al. Evidence for extrathymic changes in the T cell receptor gamma/delta repertoire. *J Exp Med* 2004; **171**: 1597–1612.
7. Gibbons DL, Haque SFY, Silberzahn T, et al. Neonates harbour highly active $\gamma\delta$ T cells with selective impairments in preterm infants. *Eur J Immunol* 2009; **39**: 1794–1806.
8. Paul S, Shilpi, Lal G. Role of gamma-delta ($\gamma\delta$) T cells in autoimmunity. *J Leukoc Biol* 2014; **97**: 259–271.
9. Dimova T, Brouwer M, Gosselin F, et al. Effector V γ 9V δ 2 T cells dominate the human fetal $\gamma\delta$ T-cell repertoire. *Proc Natl Acad Sci USA* 2015; **112**: E556–E565.
10. Godfrey DI, Uldrich AP, Mccluskey J, et al. The burgeoning family of unconventional T cells. *Nat Immunol* 2015; **16**: 1114–1124.

11. Xu W, Monaco G, Wong EH, *et al.* Mapping of γ/δ T cells reveals $V\delta 2^+$ T cells resistance to senescence. *EBioMedicine* 2019; **39**: 44–58.
12. Willcox CR, Davey MS, Willcox BE. Development and selection of the human $V\gamma 9V\delta 2^+$ T-cell repertoire. *Front Immunol* 2018; **9**: 1–7.
13. McCarthy NE, Eberl M. Human $\gamma\delta$ T-cell control of mucosal immunity and inflammation. *Front Immunol* 2018; **9**: 1–8.
14. De Rosa SC, Andrus JP, Perfetto SP, *et al.* Ontogeny of T cells in humans. *J Immunol* 2004; **172**: 1637–1645.
15. Vermijlen D, Gatti D, Kouzeli A, *et al.* $\gamma\delta$ T cell responses: how many ligands will it take till we know? *Semin Cell Dev Biol* 2018; **84**: 75–86.
16. Willcox BE, Willcox CR. $\gamma\delta$ TCR ligands: the quest to solve a 500-million-year-old mystery. *Nat Immunol* 2019; **20**: 121–128.
17. Kallemijn MJ, Boots AMH, Van Der Klift MY, *et al.* Ageing and latent CMV infection impact on maturation, differentiation and exhaustion profiles of T-cell receptor gammadelta T-cells. *Sci Rep* 2017; **7**: 1–14.
18. Willcox CR, Pitard V, Netzer S, *et al.* Cytomegalovirus and tumor stress surveillance by binding of a human $\gamma\delta$ T cell antigen receptor to endothelial protein C receptor. *Nat Immunol* 2012; **13**: 872–879.
19. Pitard V, Roumanes D, Lafarge X, *et al.* Long-term expansion of effector/memory V 2- T cells is a specific blood signature of CMV infection. *Blood* 2008; **112**: 1317–1324.
20. Huang Y, Yang Z, McGowan J, *et al.* Regulation of IgE responses by $\gamma\delta$ T cells. *Curr Allergy Asthma Rep* 2015; **15**: 1–8.
21. van den Heuvel D, Jansen MAE, Nasserinejad K, *et al.* Effects of nongenetic factors on immune cell dynamics in early childhood: the Generation R Study. *J Allergy Clin Immunol* 2017; **139**: 1923–1934.e17.
22. Morita CT, Parker CM, Brenner MB, *et al.* TCR usage and functional capabilities of human gamma delta T cells at birth. *J Immunol* 1994; **153**: 3979–3988.
23. Kalyan S, Kabelitz D. Defining the nature of human $\gamma\delta$ T cells: a biographical sketch of the highly empathetic. *Cell Mol Immunol* 2013; **10**: 21–29.
24. Olin A, Henckel E, Chen Y, *et al.* Stereotypic immune system development in newborn children. *Cell* 2018; **174**: 1277–1292.e14.
25. Stoll BJ, Hansen N, Fanaroff AA, *et al.* Late-onset sepsis in very low birth weight neonates: the experience of the NICHD Neonatal Research Network. *Pediatrics* 2002; **110**: 285–291.
26. Scheible KM, Emo J, Laniewski N, *et al.* T cell developmental arrest in former premature infants increases risk of respiratory morbidity later in infancy. *JCI Insight* 2018; **3**: 1–17.
27. Strunk T, Currie A, Richmond P, *et al.* Innate immunity in human newborn infants: prematurity means more than immaturity. *J Matern Neonatal Med* 2011; **24**: 25–31.
28. Khairallah C, Déchanet-Merville J, Capone M. $\gamma\delta$ T cell-mediated immunity to cytomegalovirus infection. *Front Immunol* 2017; **8**: 1–13.
29. Jansen MAE, van den Heuvel D, Jaddoe VWV, *et al.* Abnormalities in $CD57^+$ cytotoxic T cells and $V\delta 1^+$ $\gamma\delta$ T cells in subclinical celiac disease in childhood are affected by cytomegalovirus. The Generation R Study. *Clin Immunol* 2017; **183**: 233–239.
30. Sohlberg E, Saghafian-Hedengren S, Rasul E, *et al.* Cytomegalovirus-seropositive children show inhibition of *in vitro* EBV infection that is associated with $CD8^+CD57^+$ T cell enrichment and IFN- γ . *J Immunol* 2013; **191**: 5669–5676.
31. Van Den Heuvel D, Jansen MAE, Dik WA, *et al.* Cytomegalovirus- and epstein-barr virus-induced T-cell expansions in young children do not impair naive T-cell populations or vaccination responses: the Generation R study. *J Infect Dis* 2016; **213**: 233–242.
32. Vermijlen D, Brouwer M, Donner C, *et al.* Human cytomegalovirus elicits fetal $\gamma\delta$ T cell responses in utero. *J Exp Med* 2010; **207**: 807–821.
33. Kotsioprifitis M, Tanner JE, Alfieri C. Heat shock protein 90 expression in Epstein-Barr virus-infected B cells promotes T-cell proliferation *in vitro*. *J Virol* 2005; **79**: 7255–7261.
34. Xiang Z, Liu Y, Zheng J, *et al.* Targeted activation of human $V\gamma 9V\delta 2$ -T cells controls Epstein-Barr virus-induced B cell lymphoproliferative disease. *Cancer Cell* 2014; **26**: 565–576.
35. Nilsson C, Linde A, Montgomery SM, *et al.* Does early EBV infection protect against IgE sensitization? *J Allergy Clin Immunol* 2005; **116**: 438–444.
36. Wejryd E, Marchini G, Frimmel V, *et al.* Probiotics promoted head growth in extremely low birthweight infants in a double-blind placebo-controlled trial. *Acta Paediatr Int J Paediatr* 2019; **108**: 62–69.
37. Grillner L. Screening of blood donors for cytomegalovirus (CMV) antibodies: an evaluation of different tests. *J Virol Methods* 1987; **17**: 133–139.

SUPPORTING INFORMATION

Additional supporting information may be found online in the Supporting Information section at the end of the article.

© 2019 The Authors.
Immunology & Cell Biology published by John Wiley & Sons Australia, Ltd on behalf of Australasian Society for Immunology Inc.

This is an open access article under the terms of the Creative Commons Attribution-NonCommercial-NoDerivs License, which permits use and distribution in any medium, provided the original work is properly cited, the use is non-commercial and no modifications or adaptations are made.